

Phloem-Specific Expression of Yang Cycle Genes and Identification of Novel Yang Cycle Enzymes in *Plantago* and *Arabidopsis*

Benjamin Pommerrenig,^{a,b} Kirstin Feussner,^c Wolfgang Zierer,^a Valentyna Rabinovych,^a Franz Klebl,^a Ivo Feussner,^c and Norbert Sauer^{a,b,1}

^a Molekulare Pflanzenphysiologie, Friedrich-Alexander-Universität Erlangen-Nürnberg, D-91058 Erlangen, Germany

^b Erlangen Center of Plant Science, Friedrich-Alexander-Universität Erlangen-Nürnberg, D-91058 Erlangen, Germany

^c Abteilung Biochemie der Pflanze, Albrecht-von-Haller-Institut für Pflanzenwissenschaften, Georg-August-Universität Göttingen, 37077 Göttingen, Germany

The 5-methylthioadenosine (MTA) or Yang cycle is a set of reactions that recycle MTA to Met. In plants, MTA is a byproduct of polyamine, ethylene, and nicotianamine biosynthesis. Vascular transcriptome analyses revealed phloem-specific expression of the Yang cycle gene 5-METHYLTHIORIBOSE KINASE1 (MTK1) in *Plantago major* and *Arabidopsis thaliana*. As *Arabidopsis* has only a single MTK gene, we hypothesized that the expression of other Yang cycle genes might also be vascular specific. Reporter gene studies and quantitative analyses of mRNA levels for all Yang cycle genes confirmed this hypothesis for *Arabidopsis* and *Plantago*. This includes the Yang cycle genes 5-METHYLTHIORIBOSE-1-PHOSPHATE ISOMERASE1 and DEHYDRATASE-ENOLASE-PHOSPHATASE-COMPLEX1. We show that these two enzymes are sufficient for the conversion of methylthioribose-1-phosphate to 1,2-dihydroxy-3-keto-5-methylthiopentene. In bacteria, fungi, and animals, the same conversion is catalyzed in three to four separate enzymatic steps. Furthermore, comparative analyses of vascular and nonvascular metabolites identified Met, S-adenosyl Met, and MTA preferentially or almost exclusively in the vascular tissue. Our data represent a comprehensive characterization of the Yang cycle in higher plants and demonstrate that the Yang cycle works primarily in the vasculature. Finally, expression analyses of polyamine biosynthetic genes suggest that the Yang cycle in leaves recycles MTA derived primarily from polyamine biosynthesis.

INTRODUCTION

Based on the finding that the amount of ethylene produced in apple fruits (*Malus domestica*) largely exceeded the amount of the ethylene precursor Met, Baur and Yang (1972) suggested that the sulfur in Met has to be recycled during ethylene biosynthesis. A set of recycling reactions was proposed for plants by Miyazaki and Yang (1987), and the names Yang cycle, Met cycle, 5-methylthioadenosine (MTA) cycle, or Met-salvage pathway developed as synonyms for these reactions. Several of these reactions had been predicted due to the identification of expected intermediates; most enzymatic steps, however, were deduced from data obtained in animals and bacteria.

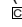
Today it is well established that the Yang cycle in plants is essential not only for ethylene biosynthesis but also for polyamine and nicotianamine/phytosiderophore biosynthetic reactions. All of these reactions use the same aminobutyrate moiety

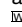
of S-adenosyl methionine (SAM; Kende, 1993; Roje, 2006) and produce MTA, which has to be recycled (Figure 1). Obviously, depending on the relative biosynthetic activities, the Yang cycle in different tissues might be involved in the recycling of MTA produced in different biosynthetic processes.

The first Yang cycle enzyme from plants, 5-methylthioribose kinase (MTK), was identified only a few years ago by Sauter et al. (2004) from rice (*Oryza sativa*; Os MTK1 and Os MTK2) and *Arabidopsis thaliana* (At MTK1). MTKs catalyze the ATP-dependent conversion of 5-methylthioribose (MTR) to 5-methylthioribose-1-phosphate (MTR-1-P; Figure 1). *Arabidopsis MTK1* (At1g49820) is the only MTK gene in the *Arabidopsis* genome, and database searches suggested that most higher plants possess only a single MTK gene. In fact, the two rice genes are located in tandem on the genome, are more than 95% identical, and were suggested to have evolved only recently via gene duplication (Sauter et al., 2004). A second plant Yang cycle enzyme, an acidoreductone oxygenase (ARD) converting 1,2-dihydro-3-keto-5-methylthiopentene (DHKMP) to 2-keto-4-methylthiobutyrate (KMTB) (Figure 1), was described by Sauter et al. (2005). Two ARD enzymes, Os ARD1 and Os ARD2, were identified in rice (Sauter et al., 2005), and four homologous sequences (ARD1 [At4g14716], ARD2 [At4g14710], ARD3 [At2g26400], and ARD4 [At5g43850]) were found in the *Arabidopsis* genome. Finally, Rzewuski et al. (2007) characterized 5-methylthioadenosine nucleosidase (MTN) as a third Yang cycle enzyme

¹ Address correspondence to nsauer@biologie.uni-erlangen.de.

The author responsible for distribution of materials integral to the findings presented in this article in accordance with the policy described in the Instructions for Authors (www.plantcell.org) is: Norbert Sauer (nsauer@biologie.uni-erlangen.de).

 Some figures in this article are displayed in color online but in black and white in the print edition.

 Online version contains Web-only data.

www.plantcell.org/cgi/doi/10.1105/tpc.110.079657

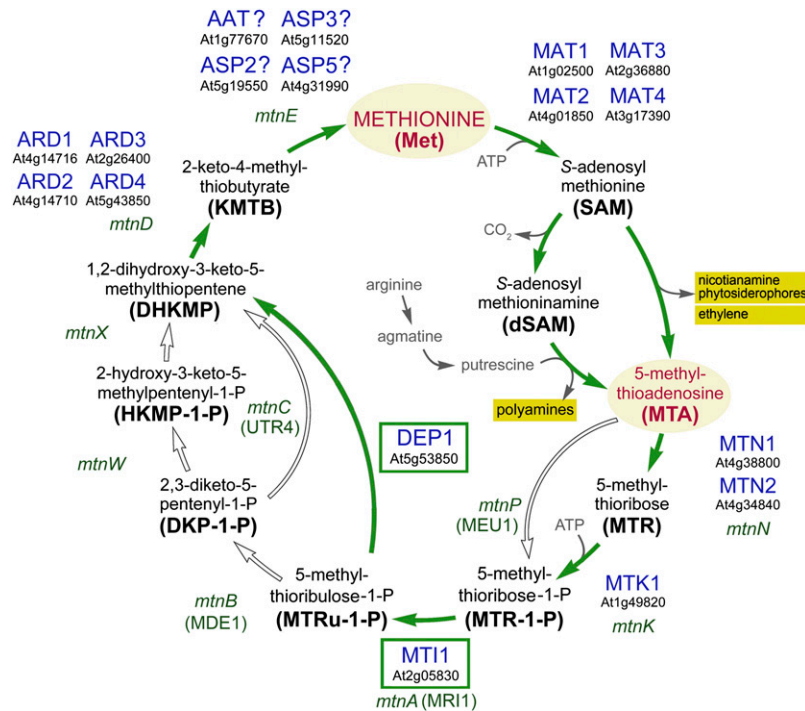


Figure 1. Yang Cycle Reactions in Bacteria, Yeast, and Plants.

Variations of Yang cycle reactions in bacteria (gene names in lowercase, italic), *S. cerevisiae* (gene names in parentheses), and plants (enzyme names with MIPS numbers). Plant enzymes identified and characterized in this article (DEP1 and MT11) are boxed. Closed arrows show reactions found in plants; open arrows show enzymes not found in plants. Met, the end product of the Yang cycle, and MTA, the common byproduct of polyamine, nicotianamine, phytosiderophore, and ethylene biosynthesis, are highlighted. Abbreviations of plant enzymes not mentioned in this article: MAT1 to MAT4, Met adenosyltransferases (=SAM synthases) 1 to 4. Question marks were added to the names of four aminotransferases that might catalyze the conversion of KMTB to Met, as direct proof for this function is still missing. [See online article for color version of this figure.]

(Figure 1). MTNs cleave adenine from MTA and produce MTR (Figure 1). Whereas only a single *MTN* gene was found in the rice genome, two homologous sequences were identified in *Arabidopsis* (*MTN1* [At4g38800] and *MTN2* [At4g34840]).

So far, the enzyme(s) catalyzing the isomerization of MTR-1-P to 5-methylthioribulose-1-P (MTRu-1-P), the enzymes responsible for the conversion of MTRu-1-P to DHKMP, and the transaminase(s) catalyzing the conversion of KMTB to Met (Figure 1) have only been characterized in bacteria, fungi, and animals. Moreover, the number of enzymes involved in the conversion of MTRu-1-P to DHKMP in plants is unclear, as alternative paths had been found in different bacteria and in *Saccharomyces cerevisiae* (baker's yeast; Figure 1; Sekowska et al., 2004).

Here, we present (1) comprehensive physiological analyses of the Yang cycle in the leaves of higher plants, (2) identification and functional characterization of the Yang cycle enzymes 5-METHYLTHIORIBOSE-1-PHOSPHATE ISOMERASE1 (MT11) and DEHYDRATASE-ENOLASE-PHOSPHATASE-COMPLEX1 (DEP1), and (3) an analysis of the reactions producing the Yang cycle substrate MTA. We demonstrate that only two enzymes, MT11 and DEP1, are involved in the catalysis of a set of reactions that is performed by three to four enzymes in bacteria, fungi, and

animals. Detailed expression studies of all Yang cycle genes in *Arabidopsis* and *Plantago major* revealed that both all previously described and the newly characterized genes are specifically or preferentially expressed in the phloem. This result is supported by comparative metabolite analyses that found Met, SAM, MTA, and the polyamines putrescine, spermine, and spermidine enriched in the leaf vasculature. Finally, comparative expression analyses of polyamine and ethylene biosynthetic genes demonstrated that polyamine biosynthesis also occurs preferentially in the vasculature. In summary, our data suggest that the primary role of the Yang cycle in the leaves of higher plants is the recycling of MTA produced during polyamine biosynthesis in the leaf vasculature. The impact of these findings on the potential roles of polyamine biosynthesis is discussed.

RESULTS

Expression of the *MTK1* Is Phloem Specific in *Arabidopsis* and *Plantago*

In transcriptome analyses of isolated leaf vascular bundles from *Plantago* (Pommerrenig et al., 2006), we identified mRNA

sequences of an *MTK1* gene (74.8% identical amino acids with *MTK1* from *Arabidopsis*). In *Plantago*, vascular tissue can easily and rapidly be isolated from mature leaves, and the remaining leaf tissue is almost devoid of vascular bundles (Gahrtz et al., 1994; Pommerrenig et al., 2006, 2007). We could show that the *Plantago MTK1* gene is expressed almost exclusively in the leaf vasculature (Pommerrenig et al., 2006; Figure 2A), and analyses of transgenic *Arabidopsis* plants that expressed the β -glucuronidase reporter gene (*GUS*) under the control of the *Arabidopsis MTK1* promoter (pAt-*MTK1*) revealed that the single *Arabidopsis MTK1* gene is also vasculature specific (Figures 2B and 2C). Moreover, leaf and petiole cross sections (Figures 2D and 2E) showed that *MTK1* is expressed mainly in the phloem part of the vasculature.

These results were unexpected, as it was generally accepted that the Yang cycle is a ubiquitously occurring set of reactions and equally active in most or even all cells of higher plants. However, supporting evidence came from a transcriptome profiling of discrete *Arabidopsis* cell populations (Mustroph et al., 2009; Translatome eFP Browser, <http://efp.ucr.edu/cgi-bin/relative.cgi>). In these analyses, the ribosomal protein L18 was FLAG tagged and expressed under the control of 13 different promoters. Resulting transformants were then used to immunopurify ribosome-associated mRNAs using antibodies against the FLAG-epitope, and based on the specificities of the promoters used, these coprecipitated mRNAs could be assigned to the translational activities of certain cell types. Among the *Arabidopsis* promoters used were the root and shoot companion cell (CC)-specific *SUC2* promoter (Truernit and Sauer, 1995; Stadler and Sauer, 1996; Imlau et al., 1999) and the root CC-specific and shoot bundle sheath-specific *SULTR2* promoter (Takahashi et al., 2000). Interestingly, Mustroph et al. (2009) noted already in the article first describing this approach that the phloem CCs had the most distinctive translomes of all cell types analyzed.

These Translatome eFP Browser data confirmed high expression levels of the *Arabidopsis MTK1* gene in phloem CCs, weak

expression in the shoot bundle sheath, and no expression in all other parts of the leaf (see Supplemental Figure 1 online).

Expression of Other Known Yang Cycle Genes Is Also Phloem Specific

As there is no second *MTK* gene in *Arabidopsis*, we hypothesized that due to the observed phloem-specific expression of this gene, the expression of other Yang cycle genes might be phloem specific as well. Besides *MTK1*, the *MTN* genes (*MTN1* and *MTN2* in *Arabidopsis*) and the *ARD* genes (*ARD1* to *ARD4* in *Arabidopsis*) were the only known Yang cycle genes in plants. In agreement with our hypothesis, the *Arabidopsis* Translatome eFP Browser predicted mostly phloem-specific expression for *MTN1* (expression was also observed in guard cells) and a highly phloem-specific expression for *ARD1*, *ARD2*, and *ARD3* (see Supplemental Figure 2 online). *MTN2* was predicted to be expressed only weakly in the phloem plus in the leaf epidermis and *ARD4* in the phloem plus in bundle sheath cells (see Supplemental Figure 2 online).

To independently confirm these predictions, we generated transgenic *Arabidopsis* lines expressing *GUS* under the control of the *Arabidopsis MTN1*, *ARD1*, *ARD2*, *ARD3*, or *ARD4* promoters (pAt-*MTN1*, pAt-*ARD1*, pAt-*ARD2*, pAt-*ARD3*, and pAt-*ARD4*). For the pAt-*ARD1*, pAt-*ARD2*, and pAt-*ARD4* constructs, the *GUS* sequence was fused in frame to the 3' end of a large genomic fragment consisting of the promoter and all introns and exons of the respective gene. For *MTN1*, the *GUS* analyses (Figure 3) confirmed the predicted phloem-specific expression in *Arabidopsis* source leaves (Figures 3A and 3B). *GUS* analyses of petiole sections demonstrated that the observed vascular specificity of pAt-*MTN1* results from promoter activity in the phloem part of the vasculature (Figure 3C).

Figure 4 shows that in agreement with the predictions of the *Arabidopsis* Translatome eFP Browser, pAt-*ARD1/GUS* (Figures

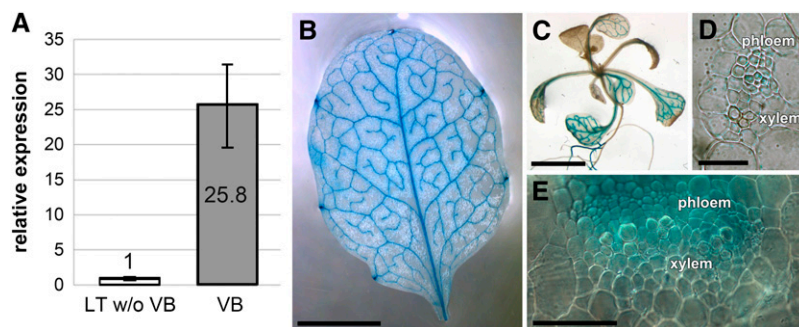


Figure 2. Vascular-Specific Expression of the *Plantago MTK1* Gene and Vascular-Specific Expression of *GUS* under the Control of pAt-*MTK1* in *Arabidopsis*.

(A) qRT-PCR analyses of Pm *MTK1* expression were performed on total RNA from isolated vascular bundles (VB) or on RNA from leaf tissue, from which all major veins had been extracted (=leaf tissue without vascular bundles [LT w/o VB]; $n = 3$; \pm SD).

(B) Source leaf of a pAt-*MTK1/GUS Arabidopsis* plant.

(C) Rosette of a pAt-*MTK1/GUS* plant.

(D) Semithin (4 μ m) microtome-cut section with *GUS* staining mainly in the phloem.

(E) Hand-cut section through the leaf vein of a pAt-*MTK1/GUS* plant showing *GUS* staining mainly in the phloem part.

Bars = 2 mm in (B) and (C) and 5 μ m in (D) and (E).

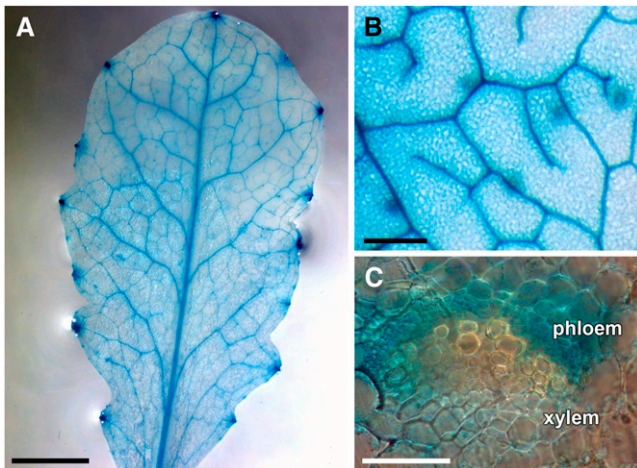


Figure 3. GUS-Histochemical Analysis of Plants Expressing the Reporter Gene under the Control of the *MTN1* Gene Promoter of *Arabidopsis*.

- (A) Source leaf of a pAt-*MTN1*/*GUS* plant.
 (B) Higher magnification of the vasculature in a different leaf.
 (C) Hand-cut section through the petiole of a pAt-*MTN1* source leaf showing GUS staining in the phloem part of the vasculature but not in the xylem.
 Bars = 1 mm in (A), 200 μ m in (B), and 5 μ m in (C).

4A and 4B), pAt-*ARD2*/*GUS* (Figure 4C), and pAt-*ARD4*/*GUS* (Figure 4F) plants clearly have vascular-specific GUS activities. In source leaves of all pAt-*ARD3*/*GUS* plants, however, the GUS staining was always (Figure 4D) patchy and pointed toward significant pAt-*ARD3* activity also outside the vasculature. Within these GUS-stained patches, however, and in cotyledons of pAt-*ARD3*/*GUS* seedlings (insert of Figure 4D), significantly stronger GUS activity was observed in the vasculature.

In the *Plantago* vascular transcriptome (Pommerrenig et al., 2006), a cDNA with strong sequence similarity to the *Arabidopsis* *ARD* genes was identified (82.29, 81.00, 74.63, and 65.59% identity on the amino acid level to At *ARD1*, At *ARD2*, At *ARD3*, and At *ARD4*, respectively). The gene was named Pm *ARD1*, and its expression in vascular bundles versus leaf tissue without vascular bundles was determined by quantitative RT-PCR (qRT-PCR). Figure 4F shows that as for the *Arabidopsis* *ARD1*, *ARD2*, and *ARD4* genes, expression of Pm *ARD1* is significantly stronger in the vasculature than in the residual leaf tissue, from which the vascular bundles had been extracted.

In summary, these analyses demonstrate that with a single exception (At *ARD3*) all analyzed *Arabidopsis* and *Plantago* *MTN*, *MTK*, and *ARD* genes show strictly or preferentially phloem-specific expression.

The Isomerization of MTR-1-P to MTRu-1-P

Enzymes catalyzing the steps between MTR-1-P, the product of MTK1, and DHKMP, the substrate of *ARD* enzymes (Figure 1), have been extensively characterized in nonplant systems. In plants, an *Arabidopsis* candidate gene (At2g05830) for the

enzyme catalyzing the isomerization of MTR-1-P to MTRu-1-P was identified by BLAST searches (<http://www.ncbi.nlm.nih.gov/blast/Blast.cgi>; this article; Sekowska et al., 2004) using as queries sequences from baker's yeast (Mri1p) or bacteria (MtnA). We named this gene *MTI1*, performed additional in silico analyses with this sequence, and tested the function of the *Arabidopsis* MTI1 protein by expressing an *MTI1* cDNA in a yeast mutant with a defect in its MTR-1-P isomerase (Δ mri1; Pirkov et al., 2008).

In publicly accessible data libraries (e.g., in The Arabidopsis Information Resource, <http://www.Arabidopsis.org/>), At2g05830 is described as a putative eukaryotic translation initiation factor eIF-2B family protein. In 2003, however, Ashida et al. (2003) characterized an eIF-2B-related (eIF-2B_{rel}) protein from *Bacillus subtilis* as an MTR-1-P isomerase. Moreover, the crystallization of the MTR-1-P isomerase from baker's yeast (Ypr118w = Mri1p, Figure 1; Bumann et al., 2004) identified sequence differences allowing a clear separation of eIF-2B translation initiation factors and MTR-1-P isomerases. In fact, phylogenetic analyses of the *Arabidopsis* MTI1 sequence, of other putative or characterized MTR-1-P isomerases, of eIF-2B_{rel} proteins, and of classical eIF-2B translation initiation factors show that the MTI1 protein clusters with functionally characterized MTR-1-P isomerases (Figure 5; see Supplemental Data Set 1 online). Moreover, MTI1 does not cluster with two other predicted *Arabidopsis* eIF-2B proteins (At1g72340 and At5g38640) that are more closely related to the well-characterized eIF-2B proteins from other species (Figure 5).

Complementation analyses with a baker's yeast strain (Y07405) that had its MTR-1-P isomerase gene (*YPR118W*) deleted (Δ mri1) confirmed this predicted function for the *Arabidopsis* MTI1 protein. Pirkov et al. (2008) demonstrated that yeast cells defective in one of their Yang cycle enzymes can grow on medium with Met as single sulfur source but not on medium with MTA as the sole sulfur source, as MTA cannot be converted to Met. Figure 6 shows that this growth defect of the Δ mri1 mutant on MTA is successfully complemented by expression of the *Arabidopsis* *MTI1* cDNA in sense orientation but not in antisense orientation. This doubtlessly characterizes the *Arabidopsis* MTI1 protein as a functional MTR-1-P isomerase.

The Conversion of MTRu-1-P to DHKMP

In bacteria, the reactions converting MTRu-1-P to DHKMP (Figure 1) are catalyzed by either three separate enzymes (MtnB, MtnW, and MtnX; e.g., in *B. subtilis*) or by only two enzymes (MtnB and MtnC; e.g., in *Klebsiella pneumoniae*) with MtnB representing a dehydratase, MtnW an enolase, MtnX a phosphatase, and MtnC a combined enolase-phosphatase (Figure 1; Sekowska et al., 2004). In baker's yeast, these reactions are also catalyzed by two enzymes (Mde1p and Utr4p; Figure 1; Pirkov et al., 2008). BLAST analyses (Sekowska et al., 2004; this article) revealed a 507-amino acid *Arabidopsis* protein, At5g53850, with sequence similarity to animal, bacterial, and fungal MtnB dehydratases in its N-terminal half (e.g., 38.36% identity of the 250 N-terminal amino acids of At5g53850 with the Mde1p dehydratase of *S. cerevisiae*; accession number P47095) and to animal, bacterial, and fungal MtnC enolase-phosphatases

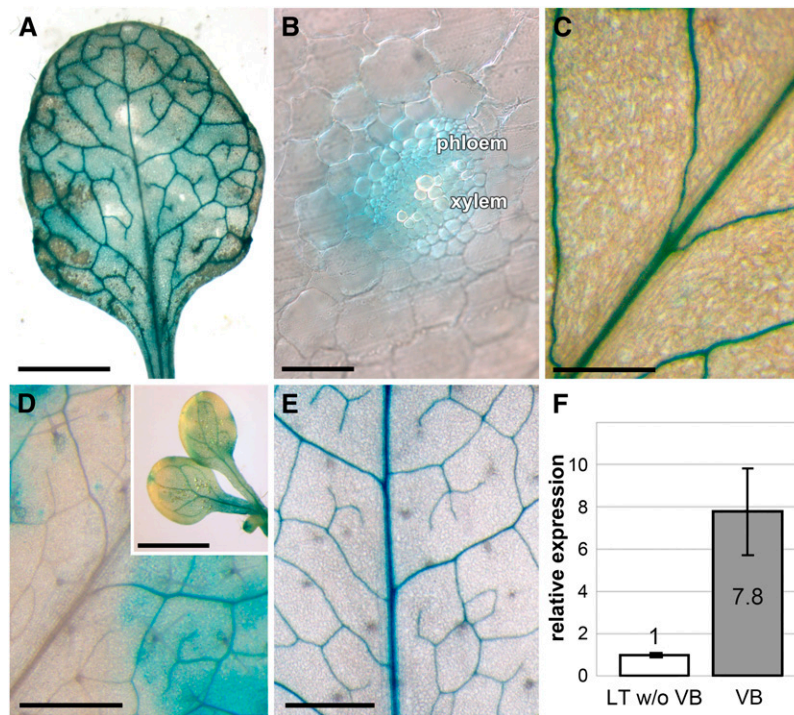


Figure 4. GUS-Histochemical Analyses of Plants Expressing the Reporter Gene under the Control of the Four Different *ARD* Gene Promoters of *Arabidopsis* and Vascular-Specific Expression of the *Plantago ARD1* Gene.

(A) Source leaf of a pAt-*ARD1*/*GUS* plant.

(B) Hand-cut section through the vascular bundle of a pAt-*ARD1*/*GUS* source leaf showing GUS staining primarily in the phloem part.

(C) GUS-stained vasculature in the source leaf of a pAt-*ARD2*/*GUS* plant.

(D) Source leaf of a pAt-*ARD3*/*GUS* plant with patchy GUS staining in the leaf blade. The inset shows cotyledons of a pAt-*ARD3*/*GUS* plant with patchy GUS activity in the background and GUS staining of the vascular bundles.

(E) GUS-stained vasculature in a source leaf of a pAt-*ARD4*/*GUS* plant.

(F) qRT-PCR analyses of Pm *ARD1* expression were performed on total RNA from isolated vascular bundles (VB) or on RNA from leaf tissue, from which all major veins had been extracted (LT w/o VB; $n = 3$; \pm SD).

Bars = 2 mm in (A), 5 μ m in (B), 250 μ m in (C), 1 mm in (D) and inset of (D), and 0.5 mm in (E).

in its C-terminal half (e.g., 40.66% identity of the 250 C-terminal amino acids of At5g53850 with the MtnC enolase/phosphatase of *Yersinia pestis*; accession number A9R2Z7). A schematic alignment of several proteins is shown in Figure 7A.

We performed separate phylogenetic studies on the N-terminal (Figure 7B; see Supplemental Data Set 2 online) and the C-terminal parts (Figure 7C; see Supplemental Data Set 3 online) of the identified *Arabidopsis* At5g53850 protein. These analyses confirmed short phylogenetic distances between the At5g53850 N terminus and characterized dehydratases and between the At5g53850 C terminus and functionally characterized enolase-phosphatases. This suggested that At5g53850 might be a fusion of a dehydratase (N terminus) and an enolase-phosphatase (C terminus). Therefore, we named the identified *Arabidopsis* gene *DEP1*.

To characterize *DEP1* as a trifunctional dehydratase-enolase-phosphatase, we used the same complementation approach as for the *MTI1* protein (see above and Figure 6). As the baker's yeast MTRu-1-P dehydratase (Mde1p) and enolase/phosphatase (Utr4p) proteins were previously characterized (Pirkov et al.,

2008; Figure 1), we could use baker's yeast strains that had their *MDE1* (YJR024C) or *UTR4* (YEL038W) genes deleted (strain Y06822 [Δ mde1] and strain Y00279 [Δ utr4]) for complementation analyses with the *Arabidopsis DEP1* cDNA.

Figure 6 demonstrates that expression of the foreign *DEP1* cDNA has a slightly negative effect on the growth of Δ mde1 and Δ utr4 cells in the presence of Met. Nevertheless, the strong growth defect of the Δ mde1 and the weaker growth defect of Δ utr4 mutants on MTA were both complemented by the expression of the *Arabidopsis DEP1* cDNA in sense orientation. Together, our results characterize *DEP1* protein as a trifunctional dehydratase/enolase/phosphatase. The data presented so far were included into the comparative overview of bacterial, yeast, and plant Yang cycle reactions shown in Figure 1.

Tissue Specificity of *MTI1* and *DEP1* Expression

When we analyzed the tissue specificity of *MTI1* and of *DEP1* expression with the *Arabidopsis* Translatome eFP Browser, both genes were predicted to be preferentially expressed in the

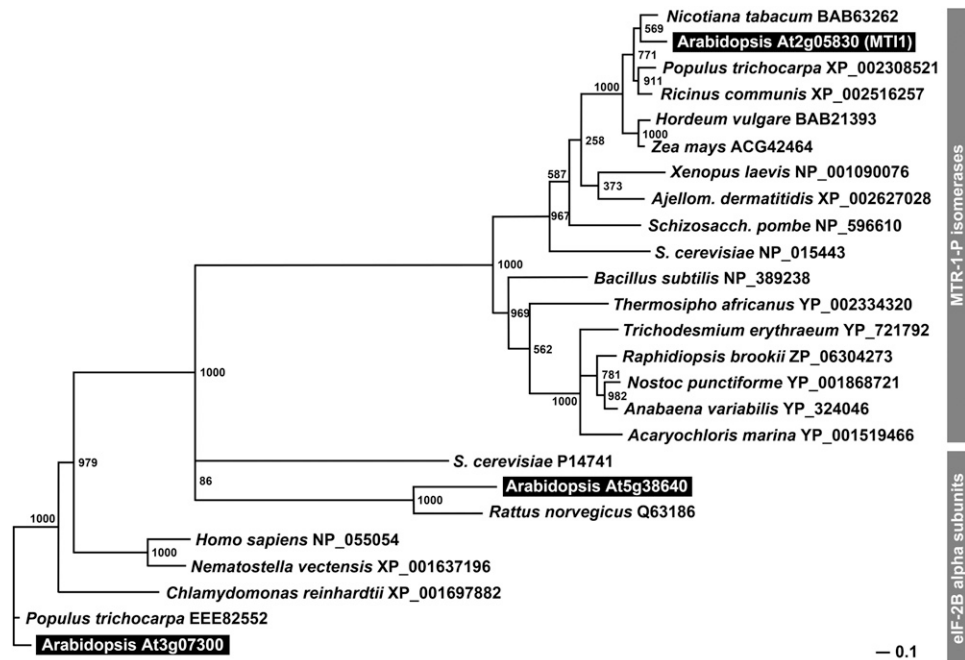


Figure 5. Phylogenetic Analyses of *Arabidopsis* MT11, of Predicted MTR-1-P Isomerases from Plants, Fungi, and Animals, and of the Closely Related α -Subunits of eIF-2B Translation Initiation Factors.

Bootstrap samples of 1000 samplings are shown at each branch. GenBank accession numbers and names of the organisms are given. *Arabidopsis* proteins are highlighted.

phloem (see Supplemental Figure 3 online). For an independent verification of these predicted patterns, we generated pAt-*MTI1*/*GUS* and pAt-*DEP1*/*GUS* reporter plants that expressed translational fusions of the *GUS* coding sequence to the 3'-ends of large genomic fragments containing promoter sequences of 1925 bp (pAt-*MTI1*) or 1649 bp (pAt-*DEP1*) plus all exons and introns of the respective gene. Analyses of the resulting pAt-*MTI1*/*GUS* and pAt-*DEP1*/*GUS* *Arabidopsis* plants showed strictly vascular specific expression of pAt-*MTI1*/*GUS* (Figure 8A) and pAt-*DEP1*/*GUS* (Figure 8B), confirming the prediction of the *Arabidopsis* Translatome eFP Browser and demonstrating that At *MTI1* and At *DEP1* show the same tissue specificity as all other Yang cycle genes.

For analyses of the expression pattern of the homologous *Plantago* genes, we cloned partial sequences of putative Pm *MTI* and Pm *DEP* genes via PCR on genomic *Plantago* DNA. Whereas only a single PCR product was obtained with the *MTI*-specific primers, two products with slightly different sizes were obtained with the *DEP*-specific primers. Sequence analyses characterized the single *MTI1* primer-derived band as a fragment of an *MTI* gene (named Pm *MTI1*; accession number FR667652; 84.7% identity to At *MTI1* on the amino acid level) and the two *DEP1* primer-derived bands as fragments of two different *DEP* genes that were named Pm *DEP1* (accession number FR667653; 86.9% identity to At *DEP1* on the amino acid level) and Pm *DEP2* (accession number FR667654; 81.8% identity to At *DEP1* on the amino acid level). The different sizes of the genomic Pm *DEP1* and Pm *DEP2* fragments resulted from different intron sequences.

With primers specific for Pm *MTI1*, Pm *DEP1*, and Pm *DEP2*, we performed qRT-PCR on RNAs isolated from vascular bundles of *Plantago* source leaves or from leaf tissue without vascular bundles. For all three genes, we observed a preferential expression in the *Plantago* vasculature (Figure 8C). In summary, these

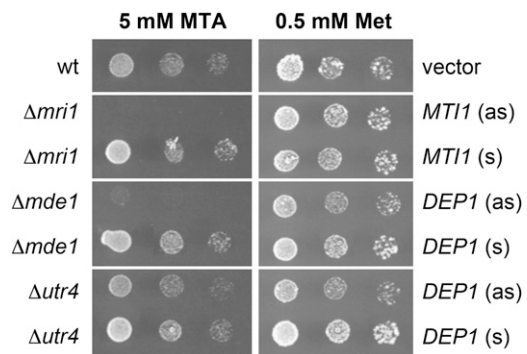


Figure 6. Comparative Growth Analyses of Wild-Type and Mutant Yeast Strains on Agar Media with MTA or Met as Sole Sources of Sulfur.

Yeast mutants defective in the Yang cycle genes *MRI1*, *MDE1*, or *UTR1* were transformed with constructs expressing the genes for the predicted *Arabidopsis* homologs either in sense (s) or in antisense (as) orientation. Expression of *MTI1* in sense but not in antisense orientation complements the growth defect of the $\Delta mri1$ mutant on MTA medium. Similarly, expression of *DEP1* in sense but not in antisense orientation complements the growth defects of $\Delta mde1$ and $\Delta utr4$ mutants on MTA medium. wt, wild type.

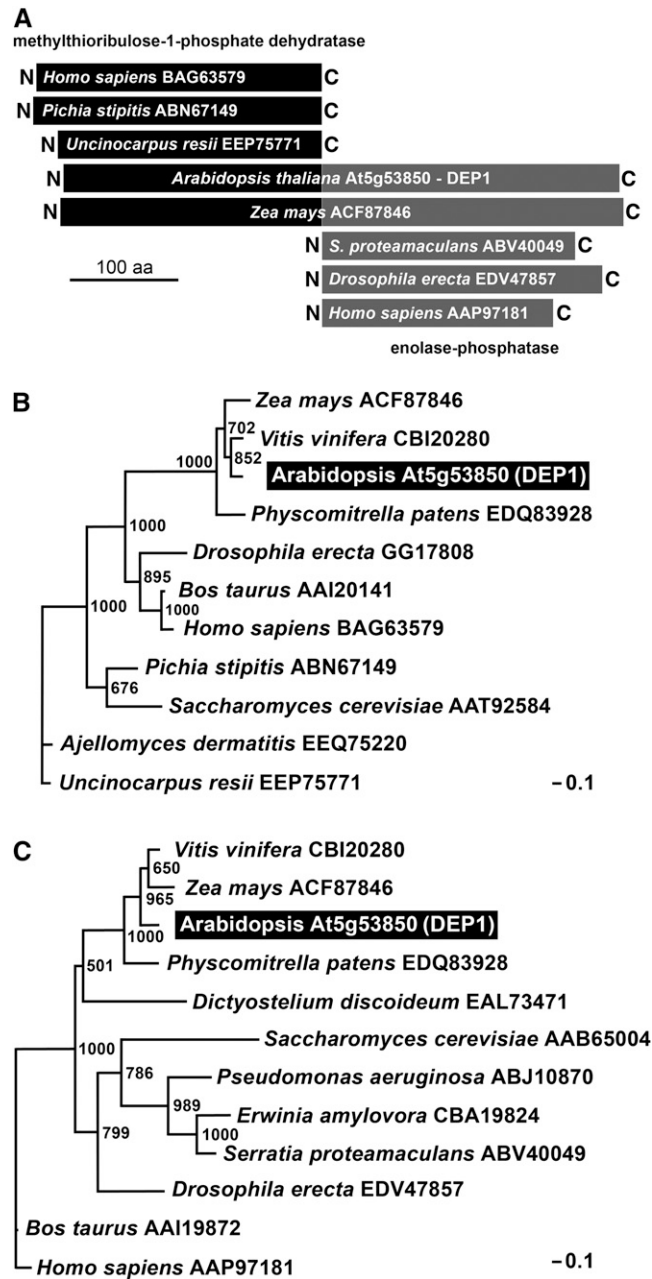


Figure 7. Phylogenetic Analyses of Plant DEP1 Proteins and Methylthioribulose-1-Phosphate Dehydratases and Enolase-Phosphatases from Other Organisms.

(A) Schematic alignment of *Arabidopsis* and maize (*Zea mays*) DEP1 proteins with characterized methylthioribulose-1-phosphate dehydratases and enolase-phosphatases from other organisms depicting the homologies of the N- and C-terminal parts of plant DEP1 proteins with the respective enzymes. aa, amino acids.

(B) Phylogenetic analysis of the N-terminal part of plant DEP1 proteins and known methylthioribulose-1-phosphate dehydratases.

(C) Phylogenetic analysis of the C-terminal domain of plant DEP1 proteins and known enolase-phosphatases.

In **(B)** and **(C)**, bootstrap samples of 1000 samplings are shown at each branch. GenBank accession numbers and names of the organisms are given. The *Arabidopsis* DEP1 protein is highlighted.

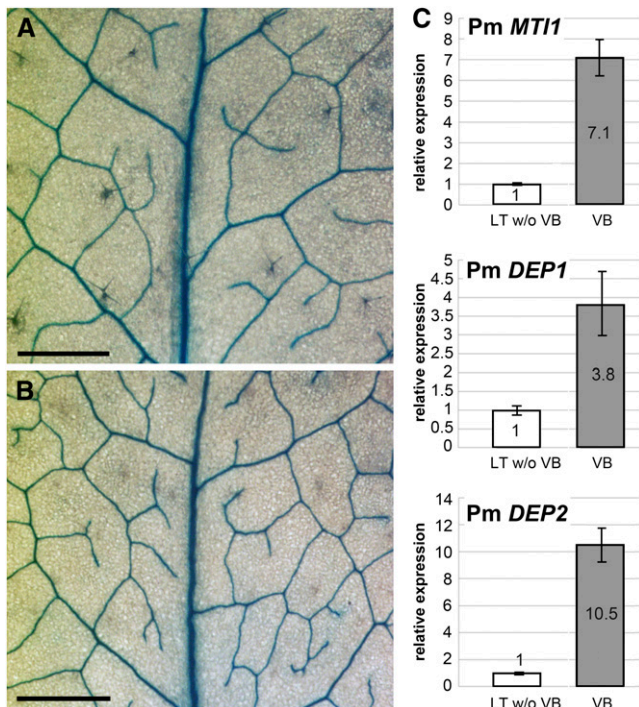


Figure 8. Vascular-Specific Expression of *Arabidopsis* and *Plantago* *MTI* and *DEP* Genes.

(A) GUS-stained vasculature in a source leaf from a pAt-*MTI1*/*GUS* plant. (B) GUS-stained vasculature in a source leaf from a pAt-*DEP1*/*GUS* plant.

(C) qRT-PCR analyses of Pm *MTI1*, Pm *DEP1*, and Pm *DEP2* expression were performed on total RNA from isolated vascular bundles (VB) or on RNA from leaf tissue, from which all major veins had been extracted (LT w/o VB; $n = 3$; \pm SD).

Bars = 0.5 mm.

[See online article for color version of this figure.]

data show that plant *DEP* and *MTI* genes are also expressed preferentially in the vasculature.

Identification of Yang Cycle Intermediates in the Vasculature of *Plantago*

We finally aimed to independently confirm the results obtained so far by biochemical data. Therefore, we performed comparative metabolite analyses on vascular and nonvascular tissue from *Plantago* source leaves. The same tissue types had already been used for the comparative qRT-PCR presented in Figures 2A, 4F, and 8C.

Figure 9A shows Box-Whisker plots of six Yang cycle metabolites or precursors of polyamine biosynthesis that were measured by ultra-performance liquid chromatography (UPLC) time-of-flight mass spectrometry (TOF-MS). The relative distributions of disaccharides and hexoses were used as markers for the biochemical purity of the preparations. As expected, disaccharides were 8-fold enriched in vascular bundles, whereas hexoses were 10-fold higher in the mesophyll (Pommerrnig

et al., 2007). Three Yang cycle metabolites, Met, SAM, and MTA, could be identified in our preparations. Whereas Met and MTA were \sim 6-fold enriched in the vasculature, the enrichment of SAM was \sim 4.5-fold. Surprisingly, Arg, a precursor of putrescine biosynthesis in *Arabidopsis* (Hanfrey et al., 2001), was \sim 60-fold enriched in the vasculature. Based on this massive enrichment of a putrescine biosynthetic precursor, we also determined the concentrations of free, perchloric acid soluble polyamines in vascular and nonvascular tissues. Figure 9B presents Box-Whisker plots for the concentrations of the polyamines putrescine, spermidine, and spermine, which had been quantified by HPLC analysis after dansylation. Although the differences were not as pronounced as for some of the Yang cycle intermediates or for Arg, all three polyamines were enriched at least 2-fold in the vasculature.

Biosynthesis of Polyamines Seems to Be the Primary Source of MTA and Feeds the Vascular Yang Cycle

Obviously, the observed phloem specificity of the Yang cycle in higher plants indicates that at least one of the three MTA-producing biosynthetic pathways (i.e., the biosynthesis of ethylene, nicotianamines/phytosiderophores, or polyamines) occurs preferentially or even exclusively in the phloem. Corroborating the observed accumulation of polyamines in the vasculature of *Plantago* (Figure 9B), we found genes for most polyamine biosynthetic steps in the *Plantago* vascular EST library (<http://www.plantain.de>), including ESTs for two SAM decarboxylases (Pm SAMDC1 [68.0% identity with At SAMDC1, At3g02470]; Pm SAMDC2: AM159097 [61.2% identity with At SAMDC1]), one *N*-carbamoylputrescine amidase (Pm CPA1 [93.4% identity with At CPA1]), one spermine synthase (Pm SPMS1 [86.8% identity with At SPMS]), and two thermo-spermine synthases (Pm ACL5A and Pm ACL5B [83.7% and 81.2% identity with At ACL5]). The reactions catalyzed by these different enzymes and the predicted expression patterns of the corresponding *Arabidopsis* genes are summarized in Supplemental Figure 4 online. Moreover, we found sequences for an ACC oxidase (Pm ACO1 [85.8% identity with At ACO, At1g05010]), a protein involved in ethylene biosynthesis. No cDNAs for proteins involved in nicotianamine biosynthesis were detected in the *Plantago* transcriptome (<http://www.plantain.de>) nor could we amplify transcripts from *Plantago* vascular mRNA using degenerate primers, an approach that was successful for the cloning of *Plantago* *MTI1* and *DEP1/DEP2* sequences.

qRT-PCR with primers specific for the identified Pm *ACO1* mRNA showed comparable expression levels of this gene in vascular and nonvascular tissue, suggesting that ethylene biosynthesis is not specific for one of the two tissues (Figure 10A). However, qRT-PCR analyses of the mRNAs of the polyamine biosynthetic enzymes revealed mainly vasculature-specific expression for Pm *SAMDC1* and significantly stronger expression in the vasculature also for Pm *SAMDC2* (Figure 10A). These enzymes catalyze the formation of *S*-adenosyl methioninamine (also decarboxylated SAM [dSAM]; Figure 1). Vasculature specificity could also be shown for the expression of the *Arabidopsis* *SAMDC2* gene, when green fluorescent protein (*GFP*) was

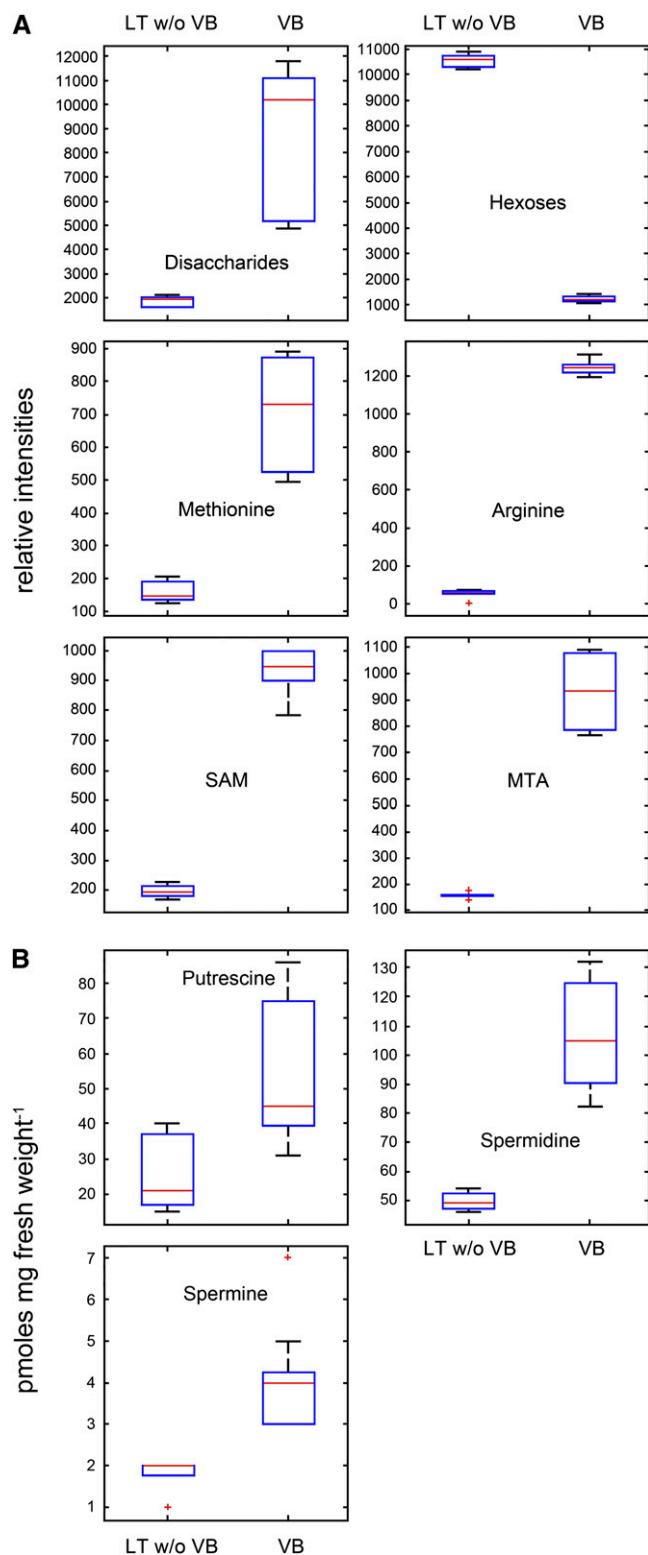


Figure 9. Relative Abundance of Yang Cycle Intermediates and Precursors or Products of Polyamine Biosynthesis in the *Plantago* Vasculature and in Vasculature-Depleted Mesophyll.

(A) Box-Whisker plots showing relative intensities of the Yang cycle

expressed under the control of the *SAMDC2* promoter (Figure 10B).

The aminopropyl moiety of dSAM is eventually transferred either to putrescine by spermidine synthases (SPDS proteins) or to spermidine by spermine or thermospermine synthases (SPMS or *ACL5* proteins, respectively; Kakehi et al., 2008; Minguet et al., 2008; see Supplemental Figure 4 online). In fact, vasculature-specific expression has only recently been demonstrated for the *SPDS2* gene from *Arabidopsis* (Hewezi et al., 2010). We also performed qRT-PCR analyses of *Plantago ACL5A*, *ACL5B*, and *SPMS1* mRNA levels and of a *Plantago N*-carbamoylputrescine amidase (*CPA1*) mRNA, which encodes the enzyme that synthesizes putrescine from *N*-carbamoylputrescine (see Supplemental Figure 4 online). Figure 10A demonstrates that the mRNA levels for all of these genes are higher in the vasculature than in nonvascular tissue; however, the difference is significantly smaller than that observed for the Yang cycle genes or for the genes encoding *SAMDC1*.

DISCUSSION

The Yang cycle in higher plants recycles MTA produced during the biosynthesis of ethylene, nicotianamine, or polyamines to Met at the expense of one ATP and of one newly added amino group. This article presents a comprehensive analysis and a detailed physiological characterization of this pathway. The work includes (1) the identification and functional characterization of the Yang cycle enzymes MTI1 and DEP1, (2) comparative expression studies of all Yang cycle genes in *Arabidopsis* and of a large set of Yang cycle genes in *Plantago* by reporter gene analyses (*Arabidopsis*) or qRT-PCR in vascular versus nonvascular tissue (*Plantago*), and (3) comparisons of the amounts of selected metabolites representing precursors of polyamine biosynthesis (Arg, Met, and SAM), Yang cycle intermediates (Met, SAM, and MTA), or products of polyamine biosynthesis. The presented data demonstrate that in contrast with bacteria, fungi, and animals, which need seven to eight enzymes for the conversion of MTA to Met, plants use only six enzymes. We show that both in *Arabidopsis* and in *Plantago*, the Yang cycle enzymes are encoded by highly vasculature-specific genes or by genes showing much stronger expression in the vasculature than in nonvascular tissue. In line with this, we found significantly higher concentrations of Met, SAM, and MTA and a less pronounced

product Met, of the Yang cycle intermediates SAM and MTA, of the polyamine biosynthetic precursor Arg, and of disaccharides and hexoses as controls (analyzed by UPLC TOF-MS measurements). VB, vascular bundles; LT w/o VB, RNA from leaf tissue, from which all major veins had been extracted; $n = 3$; \pm SD.

(B) Box-Whisker plots showing the content of free, PCA-soluble putrescine, spermidine, and spermine (quantified by HPLC analysis after dansylation). Median levels were determined from nine (polyamines) or six (all others) technical repeats of three biological replicates. Data confirming identity of the UPLC TOF-MS detected metabolites are provided as Supplemental Table 1 online.

[See online article for color version of this figure.]

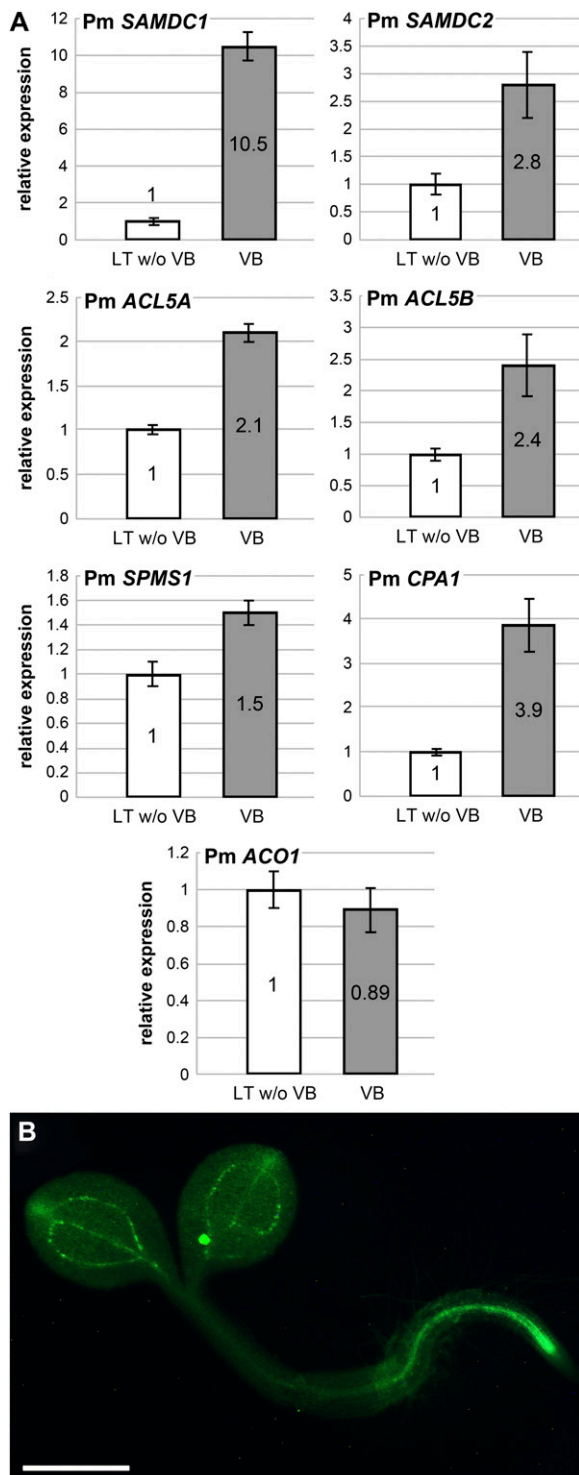


Figure 10. Vascular-Specific Expression of the *Plantago* and *Arabidopsis* Genes Involved in Polyamine and Ethylene Biosynthesis.

(A) Relative expression levels of the indicated *Plantago* genes were determined by qRT-PCR on total RNA from isolated vascular bundles (VB) or on RNA from leaf tissue, from which all major veins had been extracted (LT w/o VB; $n = 3$; \pm SD).

enrichment of polyamines in *Plantago* vascular versus nonvascular tissue and high expression levels of SAM decarboxylases in the vasculature of *Arabidopsis* and *Plantago*. Our data suggest a pivotal role of the Yang cycle in the vasculature of higher plants.

The New Yang Cycle Enzymes MTI1 and DEP1

In *Arabidopsis*, three Yang cycle enzymes (MTK1, MTI1, and DEP1) are encoded by unigenes. The Yang cycle enzymes MTI1 and DEP1 were identified by BLAST analyses and characterized by yeast complementation of yeast mutants (Figure 6).

The *Arabidopsis* MTI1 protein shows a surprising sequence similarity to the α -subunits of eukaryotic transcription initiation factor eIF-2B, and, in fact, all annotations of At2g05830 (= MTI1) describe this protein as a putative eIF-2B α -subunit (AAC95160, NP_001077883, AAM91239, and others). This unexpected similarity was also shown for MTR-1-P isomerases from other organisms. The crystal structure of the respective protein from baker's yeast (Mri1p; Bumann et al., 2004) and of eIF-2B α -subunit from human (Hiyama et al., 2009), however, identified minute but clear structural differences between MTR-1-P isomerases and eIF-2B α -subunits. This and the functional characterizations of related MTR-1-P isomerases from other organisms (Ashida et al., 2003) allowed the phylogenetic discrimination between eIF-2B α -subunits and MTR-1-P isomerases (Figure 5). The predicted enzymatic function of MTI1 was eventually confirmed by the successful complementation of a $\Delta mri1$ yeast mutant (Figure 6).

DEP1, a plant-specific protein, is a trifunctional enzyme that has dehydratase, enolase, and phosphatase activity and converts MTRu-1-P directly to DHKMP (Figure 1), possibly without releasing the intermediates DKP-1-P and HKMP-1-P. This fusion of three initially separate genes is likely to provide an advantage over the situation in bacteria with typically three separate enzymes, and in other bacteria, fungi, and animals with two enzymes, an already fused difunctional enolase-phosphatase and a still separate dehydratase (Figure 1; Sekowska et al., 2004; Pirkov et al., 2008). One advantage might be that MTA and MTR, the first Yang cycle intermediates, can be channeled more rapidly through a trifunctional complex than be metabolized by two or three separate enzymes. In fact, MTA and MTR are cytotoxic and inhibit cell proliferation at higher concentrations (Di Padova et al., 1985; Sekowska and Danchin, 2002; Ku et al., 2007). Interestingly, baker's yeast and some bacteria possess MTA phosphorylases (MtnP or Meu1p proteins) that convert MTA in a single enzymatic reaction directly to MTR-1-P (Figure 1), avoiding the production of MTR. These observations even led to the testing of MTA as chemotherapeutic agent in tumor therapy (Andreu-Pérez et al., 2010), and for the same reasons Yang cycle enzymes downstream from MTR were discussed as possible targets for new antimicrobial drugs (Sekowska and Danchin, 2002).

Alternatively, the fusion of three enzymatic activities in DEP1 might point toward high rates of MTA production in the

(B) Labeling of the vasculature in *Arabidopsis* plants expressing GFP under the control of the At SAMDC2 promoter. Bar = 0.5 mm. [See online article for color version of this figure.]

vasculature and, therefore, toward a high demand of Yang cycle activity to maintain biosynthetic activities. Detailed biochemical analyses of DEP1 will be necessary for a better understanding of this possible channeling function of DEP1.

The Conversion of KMTB to Met

For the final enzymatic step of the Yang cycle, the transamination of KMTB and the formation of Met (Figure 1), KMTB aminotransferase genes were identified in bacteria (e.g., MtnE from *B. subtilis* or *Bacillus brevis*) where these genes can be part of operons containing other Yang cycle genes (Sekowska et al., 2004). In *Pseudomonas aeruginosa* or *Escherichia coli*, however, this reaction is catalyzed by the closely related, wide-spectrum aminotransferase TyrB (Sekowska et al., 2004). MtnE and TyrB belong to the pyridoxal phosphate-dependent aspartate aminotransferase superfamily. In yeast, KMTB transamination is mediated by multiple amino acid transaminases that are mainly coupled with aromatic (Aro8p and Aro9p) and branched-chain amino acids (Bat1p and Bat2p) but also with Asp (Pirkov et al., 2008).

BLAST analyses of *Arabidopsis* sequences with MtnE and TyrB identified the prokaryotic-type AAT aminotransferase (de la Torre et al., 2006) and members of the ASP family (ASP1 to ASP5; Schultz and Coruzzi, 1995; Wilkie et al., 1996), preferably ASP2, ASP3 (both cytosolic), and ASP5 (plastidic). All of these proteins represent aspartate aminotransferases like MtnE and TyrB. BLAST analyses with yeast Bat1p or Bat2p identified *Arabidopsis* branched-chain amino transferases (BCAT1 to BCAT7). In silico analyses with the *Arabidopsis* Translatome eFP Browser did not find expression in the vasculature for any of the BCAT genes. However, phloem-specific expression is predicted for AAT, ASP2, ASP3, and ASP5 (see Supplemental Figure 5 online). The sequence similarities of these proteins, the predicted vasculature-specific expression of their genes, and their known enzymatic functions suggest that one, more, or all of these proteins might catalyze KMTB amination and Met formation in *Arabidopsis* (Figure 1). Also, in other organisms, many analogs of this final aminotransferase were described that can complement one another (Sekowska et al., 2004), a well-known property of amino acid aminotransferases (Gelfand and Steinberg, 1977).

Yang Cycle Genes Are Expressed Preferentially or Specifically in the Phloem

The GUS analyses shown in Figures 2, 3, 4, and 8 demonstrate that Yang cycle genes are expressed primarily in the leaf vasculature and preferentially in the phloem. Both the vascular specificity and the preferred expression in the phloem are predicted by the Translatome eFP Browser (Mustroph et al., 2009) for many of the analyzed proteins. Moreover, qRT-PCR analyses showed vasculature-specific expression also for the respective *Plantago* genes (Figures 2A, 4F, and 8C). Finally, comparative metabolite analyses between vascular and nonvascular tissue revealed the Yang cycle intermediates SAM and MTA as well as the Yang cycle end product Met strongly enriched in the vascular tissue (Figure 9A), which is in line with a high activity of the Yang cycle in the vasculature.

The low expression levels of the three Yang cycle unigenes in *Arabidopsis*, MTK1 (Figures 2B to 2E), MT11 (Figure 8A), and DEP1 (Figure 8B), and the low expression levels of the respective *Plantago* genes in vasculature-depleted leaf tissue (Figures 2A, 4F, and 8C) suggest only low Yang cycle activities in the mesophyll and a special need for this activity in the phloem. But which biosynthetic pathway might cause this special need? Whereas phloem-specific or vascular-specific ethylene biosynthesis is neither expected nor supported by the observed expression data of the ethylene-producing enzyme ACO1 (Figure 10B), biosynthetic activities for nicotianamine and polyamine might contribute to the production of MTA in the vasculature. However, of the four nicotianamine synthase genes of *Arabidopsis* (NAS1, At5g04950; NAS2, At5g56080; NAS3, At1g09240; and NAS4, At1g56430), the gene with the highest expression levels, NAS1, is predicted to be expressed almost ubiquitously, including the mesophyll, but not in the vasculature. NAS2 is expressed mainly in the roots of seedlings and adult plants, and one of the genes, NAS4, is predicted to be expressed more strongly in the vasculature (all expression data taken from eFP Translatome Browser and Genevestigator, <https://www.genevestigator.com/>). Thus, nicotianamine biosynthesis does not seem to occur preferentially in the leaf vasculature.

The first step specifically involved in the biosynthesis of polyamines is the decarboxylation of SAM to dSAM (Figure 1). In fact, the high levels of SAMDC gene expression in the vasculature of *Plantago* (Figure 10A) and the high expression of the SAMDC2 promoter in veins of *Arabidopsis* plants (Figure 10B) suggest a high activity vascular-specific polyamine biosynthesis. Supporting evidence comes from analyses of Yang cycle mutants. These analyses indicated that a major contribution of Yang cycle reactions to the biosynthesis of ethylene is restricted to plants naturally producing high quantities of ethylene for a prolonged period of time (e.g., rice; Bürstenbinder et al., 2007). Moreover, in rice, but not in *Arabidopsis*, expression of Yang cycle genes is induced in response to ethylene (Bürstenbinder et al., 2007). However, mutant analyses in *Arabidopsis* suggested a link between the Yang cycle and polyamine biosynthesis. MTA-grown *mtn1* mutants lacking most of their MTN activity accumulated SAM and dSAM, while the synthesis of ethylene and nicotianamine was not affected (Bürstenbinder et al., 2010).

Finally, the strong accumulation of Arg observed in the phloem (Figure 9A) points in the same direction. Arg might be actively loaded into the vasculature by the high-affinity amino acid transporter AAT1, which is rather specific for basic amino acids, or by the less specific amino acid transporter AAP2. The genes for both transporters are expressed in *Arabidopsis* leaf veins (Kwart et al., 1993; Frommer et al., 1995). In *Arabidopsis*, Arg is the sole precursor for the synthesis of agmatin and eventually of putrescine in *Arabidopsis*. Unlike all other plants studied so far, *Arabidopsis* does not possess a gene for an Orn decarboxylase and is therefore unable to use Orn for putrescine biosynthesis (Hanfrey et al., 2001). However, *Arabidopsis* has two Arg decarboxylases (ADC1 and ADC2) and ADC1, which are predicted to be expressed exclusively in the vasculature (see Supplemental Figure 4 online) and might fuel putrescine formation in this tissue.

The *ADC1* promoter is strongly activated upon chilling (Hummel et al., 2004), and polyamines and Arg decarboxylases are known to be involved in the chilling tolerance of plants (Shen et al., 2000) but also in other abiotic (salt stress: Chattopadhyay et al., 1997; Kasinathan and Wingler, 2004; Kasukabe et al., 2004; Yamaguchi et al., 2006; Moschou et al., 2008; drought stress: Capell et al., 2004; Alcázar et al., 2011) and biotic stress responses (Kumar et al., 1997; Moschou et al., 2009; Hewezi et al., 2010). However, polyamines are also important for tissue and organ development in unstressed plants. Based on extensive spatial and temporal analyses of polyamine biosynthesis and catabolism in tobacco (*Nicotiana tabacum*), it was demonstrated that polyamine metabolism affects cell division/expansion, cell cycle progression, and vascular development (Paschalidis and Roubelakis-Angelakis, 2005a). The same authors provided data suggesting that polyamines might be transported within the vasculature (Paschalidis and Roubelakis-Angelakis, 2005b).

The role of polyamines in vascular development has also been studied by Clay and Nelson (2005), who found an *Arabidopsis* mutant that they named *thickvein* (*tkv*), as it developed thicker veins in leaves and inflorescence stems. The *tkv* mutation was shown to reside in the *ACAULIS5* (*ACL5*) gene, a thermospermine synthase (see Supplemental Figure 4 online), and the phenotype of the *tkv/ac15* mutant resembles that of *Arabidopsis* mutants with impaired polar auxin transport (Przemeck et al., 1996; Deyholos et al., 2000). The authors proposed a role of polyamines in vein definition and polar auxin transport. In fact, Kakehi et al. (2008) found that a loss-of-function mutant in the *Arabidopsis* *ACL5* gene fails to produce thermospermine, an isomer of spermine (see Supplemental Figure 4 online) and that this loss of thermospermine is responsible for the phenotype of this mutant.

Based on all of these analyses, one might expect polyamines to be significantly enriched in vascular versus nonvascular tissues. In fact, Figure 9B shows increased levels of putrescine, spermidine, and spermine in the vascular of *Plantago* (Figure 10A). Obviously, polyamines produced in the vasculature for the functions discussed above might be transported to other cells or tissues where they might have signaling functions and/or might be taken up by yet uncharacterized polyamine transporters.

Our data clearly support the idea that a vascular-specific Yang cycle is important for the detoxification of MTA potentially produced during polyamine biosynthesis. Polyamines are small molecules and can easily be translocated within the vascular tissue. They might represent long-distance signals, be involved in the transport of anions, or stabilize mRNAs or small interfering RNAs. The already identified regulatory role of thermospermine may only be the first example for the important roles of polyamines in the vascular system.

METHODS

Strains and Growth Conditions

Arabidopsis thaliana plants (ecotype Columbia-0) were grown in the growth chamber on potting soil under a 16-h-light/8-h-dark regime at 22°C and 60% relative humidity. *Plantago major* plants were grown in the greenhouse under ambient conditions. Yeast strains Y00000 (wild type),

Y07405 ($\Delta mri1$), Y06822 ($\Delta mde1$), and Y00279 ($\Delta utr4$) were obtained from Euroscarf. *Agrobacterium tumefaciens* strain C58 (Deblaere et al., 1985) was used for plant transformation and *Escherichia coli* strain DH5 α (Hanahan, 1983) for all cloning steps.

Cloning of *Arabidopsis* DEP1 and MT1 cDNAs and Expression in Baker's Yeast

Arabidopsis *DEP1* and *MT1* cDNAs were amplified from RNA from *Arabidopsis* leaves using the primers AtDEP1c+1f, AtDEP1c+1524r, AtMT1c+1f, and AtMT1c+1125r (see Supplemental Table 2 online). The primers introduced *EcoRI* (*MT1*) or *NotI* (*DEP1*) cloning at both cDNA ends and inserted a 15-bp sequence (5'-AAGCTTGTAAAAGAA-3') upstream of the start-ATG known to improve the expression of foreign proteins in yeast (Stadler et al., 1995; Ramsperger-Gleixner et al., 2004). Sequenced PCR products were cloned into the yeast/*E. coli* shuttle vectors NEV-E (*MT1*) or NEV-N (*DEP1*). The resulting plasmids were named NEV-E/*MT1*s and NEV-N/*DEP1*s, if they carried the cDNA inserts in sense orientation, and NEV-E/*MT1*as and NEV-N/*DEP1*as, if they carried the cDNA inserts in antisense orientation.

Yeast Transformation and Complementation Analyses

Yeast strain Y07405 ($\Delta mri1$) was transformed with the plasmids NEV-E/*MT1*s or NEV-E/*MT1*as and strains Y06822 ($\Delta mde1$) and Y00279 ($\Delta utr4$) with the plasmids NEV-N/*DEP1*s or NEV-N/*DEP1*as using the method of Gietz et al. (1992). For complementation analyses, cells were grown on minimal medium supplemented with Met (final concentration: 0.5 mM; added from a 100 \times stock in water) or MTA (final concentration: 5 mM; added from a 100 \times stock in DMSO).

Amplification of *Plantago* MT1, DEP1, and DEP2 cDNA and Genomic and cDNA Sequences

Plantago *MT1*, *DEP1*, and *DEP2* sequences were amplified from genomic DNA isolated from *Plantago* leaf tissue using degenerate primers that start at positions 512 (PmMT11-fwd2) and 1003 (PmMT11-rev3) in the coding sequence of the *Arabidopsis* *MT1* cDNA and at positions 331 (PmDEP1/2-fwd1) and 669 (PmDEP1/2-rev1) in the coding sequence of the *Arabidopsis* *DEP1* cDNA. To confirm the introns in these genomic sequences, cDNAs were amplified from vascular tissue total RNA using the primers PmMT11c-f, PmMT11c-r, PmDEP1/2c-f, and PmDEP1/2c-r, inserted into the TOPO-Zero blunt II vector (Invitrogen), and sequenced with the insert-flanking primers TOPO-1 and TOPO-2.

Isolation of Vascular and Nonvascular Tissue from *Plantago*, RNA Isolation, and mRNA Quantification by qRT-PCR

Vascular tissue and leaf tissue without vascular bundles was obtained from *Plantago* petioles as published (Gahrtz et al., 1994). Total RNA was extracted with the Trizol method (Invitrogen). cDNA synthesis was performed with 1 μ g of total RNA from either vascular or mesophyll tissue with the QuantiTect reverse transcription kit (Qiagen). qRT-PCR runs were performed on a Rotor Gene 2000 (Corbett Research). The QuantiTect SYBR Green PCR kit (Qiagen) was used for the real-time PCR reactions. qRT-PCR data were normalized to the expression of the *Plantago* *ALDP1* gene (fructose-1,6-bisphosphat-aldolase) as described (Pommerrenig et al., 2007). The following primers were used for qPCR-measurements: PmTUA-5 and PmTUA-3 for the creation of the standard curve with a pBLUESCRIPT-SK(-) vector with a cloned PmTUA2-cDNA insert.

Construction of Reporter Gene Lines and Confocal Imaging

Promoter and/or promoter gene fragments of At *ARD1*, At *ARD2*, At *ARD3*, At *ARD4*, At *DEP1*, At *MT1*, and At *MTN1* were amplified from

genomic *Arabidopsis* Columbia-0 DNA with the Phusion polymerase (New England Biolabs). The promoter fragment of the *At MTK* gene was amplified with Pwo-Polymerase (Roche Diagnostics). The following primers were used: AtARD1p-f and AtARD1-r for the amplification of the 3018-bp *At ARD1* promoter gene fragment (1638-bp promoter sequence), AtARD2p-f and AtARD2-r (for the 2921-bp *At ARD2* promoter gene fragment (1230-bp promoter sequence), AtARD3p-f and AtARD3p-r for the 1617-bp *At ARD3* promoter, AtARD4p-f and AtARD4-r for the 3212-bp *At ARD4* promoter gene fragment (1271-bp promoter sequence), AtDEP1-1649f and AtDEP1+3660r for the 5309-bp *At DEP1* promoter gene fragment (1649-bp promoter sequence), AtMTI1-1925f and AtMTI1+2078r for the 3003-bp *At MTI1* promoter gene fragment (1925-bp promoter sequence), AtMTKp-f and AtMTKp-r for the 1220-bp *At MTK* promoter, AtMTN1p-f and AtMTN1p-r for the 1321-bp *At MTN1* promoter, and AtSAMDC2-1231f and AtSAMDC2-1r for the 1231-bp *At SAMDC2* promoter.

PCR products were cloned into the Gateway Entry vector pENTR/D-TOPO (Invitrogen) or into the TOPO-Zero Blunt II vector (Invitrogen); only *AtMTK* and sequenced. Correct Entry clones were gateway cloned by LR reaction (Clonase mix; Invitrogen) into the pMDC162 or pMDC163 vectors (Invitrogen) or into the pMDC206 vector (Invitrogen) for the pAt-SAMDC2/GFP fusion. The *At MTK* promoter fragment was excised from the TOPO-Zero Blunt II vector and cloned into the *Xba*I and *Nco*I sites of the plant transformation vector pAF16 (Stadler et al., 2005). Transgenic lines were selected on Murashige and Skoog hygromycin plates and transferred onto potting soil.

GFP fluorescence in pAt-SAMDC2/GFP plants was visualized with a Leica TCS SP11 confocal microscope (Leica Microsystems) as described (Stadler et al., 2005).

Metabolite Analyses

For comparison of the relative amounts of disaccharides, hexoses, Met, Arg, SAM, and MTA between mesophyll and vascular bundles, three biological replicates of each sample were extracted using a two-phase extraction with methyl *tert*-butylether according to Matyash et al. (2008). Further analyses were performed twice for each extract by UPLC (Acquity UPLC system; Waters) coupled with an orthogonal TOF-MS (LCT Premier; Waters). For liquid chromatography, an Acquity UPLC BEH Shield RP18 column (1 × 100 mm, 1.7- μ m particle size; Waters) was used at a temperature of 40°C, at a flow rate of 0.2 mL/min, and with the following gradient for the analysis of the polar phase: 0 to 0.5 min 0% B, 0.5 to 3 min from 0% B to 20% B, 3 to 6 min from 20% B to 99% B, 6 to 9.5 min 99% B, and 9.5 to 13 min 40% B (solvent system A: water/methanol/acetonitrile/formic acid [90:5:5:0.1, v/v/v/v]; B: acetonitrile/formic acid [100:0.1, v/v]). The unpolar phase was analyzed with the equal solvent system using the following gradient: 0 to 0.5 min 40% B, 0.5 to 5.5 min from 40% B to 100% B, 5.5 to 10 min 100% B, and 10 to 13 min 40% B. The TOF-MS was operated in W optics with a mass resolution larger than 10,000 in negative and positive electrospray ionization mode. Data were acquired with MassLynx4.1 software (Waters) in centroided format over a mass-to-charge range of 50 to 1200 with scan duration of 0.5 s and an interscan delay of 0.1 s. The capillary and the cone voltage were maintained at 2700 and 30 V and the desolvation and source temperature at 250 and 80°C, respectively. Nitrogen was used as cone gas (30 L/h⁻¹) and desolvation gas (600 L/h⁻¹). For accurate mass measurement, the dynamic range enhancement mode was used for data recording. All analyses were monitored using Leu-enkephaline ([M+H]⁺ 556.2771 or [M-H]⁻ 554.2615 as well as the respective ¹³C isotopomers [M+H]⁺ 557.2804 or [M-H]⁻ 555.2648; Sigma-Aldrich) as lock spray reference compound at a concentration of 0.5 μ g/mL in acetonitrile/water (50:50, v/v) and a flow rate of 30 μ L/min. The raw mass spectrometry data were processed by the MarkerLynx application manager (Waters).

The identities of Met and SAM were confirmed by exact mass and coelution with commercially available standards. The identity of MTA was supported by exact mass and the ratios of the C12/C13 and the S32/S34 isotopomers.

The identities of disaccharide, hexose, and Arg were confirmed by tandem mass spectrometry fragment information. For that, samples were analyzed by UPLC (conditions as described above) coupled to an Applied Biosystems 4000 hybrid triple quadrupole/linear ion trap MS (MDS Sciex). Nano-electrospray ionization (nanoESI) analysis was achieved by a chip ion source (TriVersa NanoMate; Advion BioSciences). For stable nanoESI, 100 μ L min⁻¹ of 2-propanol/acetonitrile/water/formic acid (70:20:10:0.1, v/v/v/v) delivered by a 2150 HPLC pump (LKB) were added just after the column via a mixing tee valve. Using another post column splitter, 460 nL min⁻¹ of the eluent was directed to the nanoESI chip. Ionization voltage was set to \pm 1.7 kV. Disaccharide and hexose were ionized in negative and Arg in positive nanoESI mode and determined in tandem MS mode. The parameters for enhanced product ion scans were set as follows: declustering potential \pm 74 V and collision energy from \pm 10 up to \pm 30 V. The MS was operated under Analyst 1.5. The obtained fragmentation patterns were compared with the corresponding fragment information of the databases NIST 08 mass spectral library (National Institute of Standards and Technology) and MassBank (Keio University).

For the analysis of free polyamines, 100 mg homogenized plant material was mixed with 400 μ L 5% (v/v) perchloric acid (PCA) and extracted for 1 h on ice. As internal standard 1,7-heptanediamine was added. After centrifugation, PCA-soluble polyamines in the supernatant were dansylated according to Flores and Galston (1982). For quantification, the HPLC method of Minocha et al. (1990) was adapted. Putrescine, spermidine, and spermine were identified using authentic standards (all chemicals from Sigma-Aldrich).

Phylogenetic Analyses

The sequences used to calculate the phylogenetic tree shown in Figure 1 were aligned with ClustalW2 (<http://www.ebi.ac.uk/Tools/clustalw2/index.html>) using the default settings (Gonnet matrix, gap open penalty = 10.0, gap extension penalty 1 = 0.2, protein ENDGAP = -1, and protein GAPDIST = 4). Results were stored in the PHYLIP output format and used to construct an unrooted phylogenetic tree by the maximum likelihood method using the online version of PhyML 3.0 (Guindon and Gascuel, 2003) provided by Los Alamos National Security (<http://www.hiv.lanl.gov/content/sequence/PHYML/interface.html>) with the JTT model for amino acid substitutions and 1000 bootstrap samplings. TreeViewX 0.4.1 for Mac (Page, 1996) was used for tree viewing. The alignments used for tree calculation are shown in the Supplemental Data Sets 1 to 3 online.

Accession Numbers

Sequence data from this article can be found in the Arabidopsis Genome Initiative or GenBank/EMBL databases under the following accession numbers: *At AAT* (At1g77670), *At ACL5* (At5g19530), *At ARD1* (At4g14716), *At ARD2* (At4g14710), *At ARD3* (At2g26400), *At ARD4* (At5g43850), *At ASP2* (At5g19550), *At ASP3* (At5g11520), *At ASP5* (At4g31990), *At CPA1* (At2g27450), *At DEP1* (At5g53850), *At MTI1* (At2g05830), *At MTK1* (At1g49820), *At MTN1* (At4g38800), *At MTN2* (At4g34840), *At SAMDC1* (At3g02470), *At SAMDC2* (At3g25570), *At SAMDC3* (At5g15950), *At SAMDC4* (At5g18930), *At SPMS* (At5g53120), *Pm ACL5A* (AM158911), *Pm ACL5B* (AM158912), *Pm ACO1* (AJ843131), *Pm ARD1* (AM404079), *Pm CPA1* (FR667651), *Pm DEP1* (FR667653), *Pm DEP2* (FR667654), *Pm MTI1* (FR667652), *Pm MTK1* (AM113865), *Pm SAMDC1* (AM156953), and *Pm SPMS1* (AM158913).

Supplemental Data

The following materials are available in the online version of this article.

Supplemental Figure 1. Prediction of Phloem-Specific *MTK1* Expression in *Arabidopsis* Shoots and Roots.

Supplemental Figure 2. Predictions of the Phloem-Specific Expression of *MTN* and *ARD* Genes in *Arabidopsis* Shoots.

Supplemental Figure 3. Predictions of the Expression Pattern of *MT11* and *DEP1* in *Arabidopsis* Shoots.

Supplemental Figure 4. Polyamine Biosynthesis and Polyamine Biosynthetic Enzymes in *Arabidopsis*.

Supplemental Figure 5. Predictions of the Expression Patterns of Transaminases Potentially Involved in the Formation of Met from KMTB in the *Arabidopsis* Vasculature.

Supplemental Table 1. Data Confirming Identification of Differentially Accumulating Metabolites.

Supplemental Table 2. Oligonucleotide Primers Used in This Study.

Supplemental Data Set 1. Alignment (ClustalW) of the Sequences Used to Calculate the Phylogenetic Tree Shown in Figure 5.

Supplemental Data Set 2. Alignment (ClustalW) of the Sequences Used to Calculate the Phylogenetic Tree Shown in Figure 7B.

Supplemental Data Set 3. Alignment (ClustalW) of the Sequences Used to Calculate the Phylogenetic Tree Shown in Figure 7C.

ACKNOWLEDGMENTS

We thank Marina Henneberg, Cornelia Herrfurth, and Pia Meyer for help with the experiments.

Received September 20, 2010; revised March 14, 2011; accepted April 15, 2011; published May 3, 2011.

REFERENCES

- Alcázar, R., Bitrián, M., Bartels, D., Koncz, C., Altabella, T., and Tiburcio, A.F. (2011). Polyamine metabolic canalization in response to drought stress in *Arabidopsis* and the resurrection plant *Craterostigma plantagineum*. *Plant Signal. Behav.*, in press.
- Andreu-Pérez, P., Hernandez-Losa, J., Moliné, T., Gil, R., Grueso, J., Pujol, A., Cortés, J., Avila, M.A., and Recio, J.A. (2010). Methylthioadenosine (MTA) inhibits melanoma cell proliferation and in vivo tumor growth. *BMC Cancer* **10**: 265.
- Ashida, H., Saito, Y., Kojima, C., Kobayashi, K., Ogasawara, N., and Yokota, A. (2003). A functional link between RuBisCO-like protein of *Bacillus* and photosynthetic RuBisCO. *Science* **302**: 286–290.
- Baur, A.H., and Yang, S.F. (1972). Methionine metabolism in apple tissue in relation to ethylene biosynthesis. *Phytochemistry* **11**: 3207–3214.
- Bumann, M., Djafarzadeh, S., Oberholzer, A.E., Bigler, P., Altmann, M., Trachsel, H., and Baumann, U. (2004). Crystal structure of yeast Ypr118w, a methylthioribose-1-phosphate isomerase related to regulatory eIF2B subunits. *J. Biol. Chem.* **279**: 37087–37094.
- Bürstenbinder, K., Rzewuski, G., Wirtz, M., Hell, R., and Sauter, M. (2007). The role of methionine recycling for ethylene synthesis in *Arabidopsis*. *Plant J.* **49**: 238–249.
- Bürstenbinder, K., Waduware, I., Schoor, S., Moffatt, B.A., Wirtz, M., Minocha, S.C., Oppermann, Y., Bouchereau, A., Hell, R., and Sauter, M. (2010). Inhibition of 5'-methylthioadenosine metabolism in the Yang cycle alters polyamine levels, and impairs seedling growth and reproduction in *Arabidopsis*. *Plant J.* **62**: 977–988.
- Capell, T., Bassie, L., and Christou, P. (2004). Modulation of the polyamine biosynthetic pathway in transgenic rice confers tolerance to drought stress. *Proc. Natl. Acad. Sci. USA* **101**: 9909–9914.
- Chattopadhyay, M.K., Gupta, S., Sengupta, D.N., and Ghosh, B. (1997). Expression of arginine decarboxylase in seedlings of indica rice (*Oryza sativa* L.) cultivars as affected by salinity stress. *Plant Mol. Biol.* **34**: 477–483.
- Clay, N.K., and Nelson, T. (2005). *Arabidopsis thickvein* mutation affects vein thickness and organ vascularization, and resides in a provascular cell-specific spermine synthase involved in vein definition and in polar auxin transport. *Plant Physiol.* **138**: 767–777.
- Deblaere, R., Bytebier, B., De Greve, H., Deboeck, F., Schell, J., Van Montagu, M., and Leemans, J. (1985). Efficient octopine Ti plasmid-derived vectors for *Agrobacterium*-mediated gene transfer to plants. *Nucleic Acids Res.* **13**: 4777–4788.
- de la Torre, F., De Santis, L., Suárez, M.F., Crespillo, R., and Cánovas, F.M. (2006). Identification and functional analysis of a prokaryotic-type aspartate aminotransferase: Implications for plant amino acid metabolism. *Plant J.* **46**: 414–425.
- Deyholos, M.K., Corder, G., Beebe, D., and Sieburth, L.E. (2000). The SCARFACE gene is required for cotyledon and leaf vein patterning. *Development* **127**: 3205–3213.
- Di Padova, F., Di Padova, C., Stramentinoli, G., and Tritapepe, R. (1985). Inhibition of lymphocyte function by a naturally occurring nucleoside: 5'-Methylthioadenosine (MTA). *Int. J. Immunopharmacol.* **7**: 193–198.
- Flores, H.E., and Galston, A.W. (1982). Analysis of polyamines in higher plants by high performance liquid chromatography. *Plant Physiol.* **69**: 701–706.
- Frommer, W.B., Hummel, S., Unseld, M., and Ninnemann, O. (1995). Seed and vascular expression of a high-affinity transporter for cationic amino acids in *Arabidopsis*. *Proc. Natl. Acad. Sci. USA* **92**: 12036–12040.
- Gahrtz, M., Stolz, J., and Sauer, N. (1994). A phloem-specific sucrose-H⁺ symporter from *Plantago major* L. supports the model of apoplastic phloem loading. *Plant J.* **6**: 697–706.
- Gelfand, D.H., and Steinberg, R.A. (1977). *Escherichia coli* mutants deficient in the aspartate and aromatic amino acid aminotransferases. *J. Bacteriol.* **130**: 429–440.
- Gietz, D., St Jean, A., Woods, R.A., and Schiestl, R.H. (1992). Improved method for high efficiency transformation of intact yeast cells. *Nucleic Acids Res.* **20**: 1425.
- Guindon, S., and Gascuel, O. (2003). A simple, fast, and accurate algorithm to estimate large phylogenies by maximum likelihood. *Syst. Biol.* **52**: 696–704.
- Hanahan, D. (1983). Studies on transformation of *Escherichia coli* with plasmids. *J. Mol. Biol.* **166**: 557–580.
- Hanfrey, C., Sommer, S., Mayer, M.J., Burtin, D., and Michael, A.J. (2001). *Arabidopsis* polyamine biosynthesis: Absence of ornithine decarboxylase and the mechanism of arginine decarboxylase activity. *Plant J.* **27**: 551–560.
- Hewezi, T., Howe, P.J., Maier, T.R., Hussey, R.S., Mitchum, M.G., Davis, E.L., and Baum, T.J. (2010). *Arabidopsis* spermidine synthase is targeted by an effector protein of the cyst nematode *Heterodera schachtii*. *Plant Physiol.* **152**: 968–984.
- Hiyama, T.B., Ito, T., Imataka, H., and Yokoyama, S. (2009). Crystal structure of the alpha subunit of human translation initiation factor 2B. *J. Mol. Biol.* **392**: 937–951.

- Hummel, I., Bourdais, G., Gouesbet, G., Couée, I., Malmberg, R.L., and El Amrani, A. (2004). Differential gene expression of *ARGININE DECARBOXYLASE ADC1* and *ADC2* in *Arabidopsis thaliana*: Characterization of transcriptional regulation during seed germination and seedling development. *New Phytol.* **163**: 519–531.
- Imlau, A., Truernit, E., and Sauer, N. (1999). Cell-to-cell and long-distance trafficking of the green fluorescent protein in the phloem and symplastic unloading of the protein into sink tissues. *Plant Cell* **11**: 309–322.
- Takehi, J., Kuwashiro, Y., Niitsu, M., and Takahashi, T. (2008). Thermospermine is required for stem elongation in *Arabidopsis thaliana*. *Plant Cell Physiol.* **49**: 1342–1349.
- Kasinathan, V., and Wingler, A. (2004). Effect of reduced arginine decarboxylase activity on salt tolerance and on polyamine formation during salt stress in *Arabidopsis thaliana*. *Physiol. Plant.* **121**: 101–107.
- Kasukabe, Y., He, L., Nada, K., Misawa, S., Ihara, I., and Tachibana, S. (2004). Overexpression of spermidine synthase enhances tolerance to multiple environmental stresses and up-regulates the expression of various stress-regulated genes in transgenic *Arabidopsis thaliana*. *Plant Cell Physiol.* **45**: 712–722.
- Kende, H. (1993). Ethylene biosynthesis. *Annu. Rev. Plant Physiol. Plant Mol. Biol.* **44**: 283–307.
- Ku, S.-Y., Cornell, K.A., and Howell, P.L. (2007). Structure of *Arabidopsis thaliana* 5-methylthioribose kinase reveals a more occluded active site than its bacterial homolog. *BMC Struct. Biol.* **7**: 70.
- Kumar, A., Altabella, T., Taylor, M., and Tiburcio, A.F. (1997). Recent advances in polyamine research. *Trends Plant Sci.* **2**: 124–130.
- Kwart, M., Hirner, B., Hummel, S., and Frommer, W.B. (1993). Differential expression of two related amino acid transporters with differing substrate specificity in *Arabidopsis thaliana*. *Plant J.* **4**: 993–1002.
- Matyash, V., Liebisch, G., Kurzchalia, T.V., Shevchenko, A., and Schwudke, D. (2008). Lipid extraction by methyl-tert-butyl ether for high-throughput lipidomics. *J. Lipid Res.* **49**: 1137–1146.
- Minguet, E.G., Vera-Sirera, F., Marina, A., Carbonell, J., and Blázquez, M.A. (2008). Evolutionary diversification in polyamine biosynthesis. *Mol. Biol. Evol.* **25**: 2119–2128.
- Minocha, S., Minocha, R., and Robie, C. (1990). High-performance liquid chromatographic method for the determination of dansyl-polyamines. *J. Chromatogr. A* **511**: 177–183.
- Miyazaki, J.H., and Yang, S.F. (1987). Metabolism of 5-methylthioribose to methionine. *Plant Physiol.* **84**: 277–281.
- Moschou, P.N., Paschalidis, K.A., Delis, I.D., Andriopoulou, A.H., Lagiotis, G.D., Yakoumakis, D.I., and Roubelakis-Angelakis, K.A. (2008). Spermidine exodus and oxidation in the apoplast induced by abiotic stress is responsible for H₂O₂ signatures that direct tolerance responses in tobacco. *Plant Cell* **20**: 1708–1724.
- Moschou, P.N., Sarris, P.F., Skandalis, N., Andriopoulou, A.H., Paschalidis, K.A., Panopoulos, N.J., and Roubelakis-Angelakis, K.A. (2009). Engineered polyamine catabolism preinduces tolerance of tobacco to bacteria and oomycetes. *Plant Physiol.* **149**: 1970–1981.
- Mustroph, A., Zanetti, M.E., Jang, C.J.H., Holtan, H.E., Repetti, P.P., Galbraith, D.W., Girke, T., and Bailey-Serres, J. (2009). Profiling transcriptomes of discrete cell populations resolves altered cellular priorities during hypoxia in *Arabidopsis*. *Proc. Natl. Acad. Sci. USA* **106**: 18843–18848.
- Page, R.D.M. (1996). TreeView: An application to display phylogenetic trees on personal computers. *Comput. Appl. Biosci.* **12**: 357–358.
- Paschalidis, K.A., and Roubelakis-Angelakis, K.A. (2005a). Spatial and temporal distribution of polyamine levels and polyamine anabolism in different organs/tissues of the tobacco plant. Correlations with age, cell division/expansion, and differentiation. *Plant Physiol.* **138**: 142–152.
- Paschalidis, K.A., and Roubelakis-Angelakis, K.A. (2005b). Sites and regulation of polyamine catabolism in the tobacco plant. Correlations with cell division/expansion, cell cycle progression, and vascular development. *Plant Physiol.* **138**: 2174–2184.
- Pirkov, I., Norbeck, J., Gustafsson, L., and Albers, E. (2008). A complete inventory of all enzymes in the eukaryotic methionine salvage pathway. *FEBS J.* **275**: 4111–4120.
- Pommerrenig, B., Barth, I., Niedermeier, M., Kopp, S., Schmid, J., Dwyer, R.A., McNair, R.J., Klebl, F., and Sauer, N. (2006). Common plantain. A collection of expressed sequence tags from vascular tissue and a simple and efficient transformation method. *Plant Physiol.* **142**: 1427–1441.
- Pommerrenig, B., Papini-Terzi, F.S., and Sauer, N. (2007). Differential regulation of sorbitol and sucrose loading into the phloem of *Plantago major* in response to salt stress. *Plant Physiol.* **144**: 1029–1038.
- Przemeck, G.K.H., Mattsson, J., Hardtke, C.S., Sung, Z.R., and Berleth, T. (1996). Studies on the role of the *Arabidopsis* gene *MONOPTEROS* in vascular development and plant cell axialization. *Planta* **200**: 229–237.
- Ramsperger-Gleixner, M., Geiger, D., Hedrich, R., and Sauer, N. (2004). Differential expression of sucrose transporter and polyol transporter genes during maturation of common plantain companion cells. *Plant Physiol.* **134**: 147–160.
- Roje, S. (2006). S-Adenosyl-L-methionine: Beyond the universal methyl group donor. *Phytochemistry* **67**: 1686–1698.
- Rzewuski, G., Cornell, K.A., Rooney, L., Bürstenbinder, K., Wirtz, M., Hell, R., and Sauter, M. (2007). *OsMTN* encodes a 5'-methylthioadenosine nucleosidase that is up-regulated during submergence-induced ethylene synthesis in rice (*Oryza sativa* L.). *J. Exp. Bot.* **58**: 1505–1514.
- Sauter, M., Cornell, K.A., Beszteri, S., and Rzewuski, G. (2004). Functional analysis of methylthioribose kinase genes in plants. *Plant Physiol.* **136**: 4061–4071.
- Sauter, M., Lorbiecke, R., Ouyang, B., Pochapsky, T.C., and Rzewuski, G. (2005). The immediate-early ethylene response gene *OsARD1* encodes an acireductone dioxygenase involved in recycling of the ethylene precursor S-adenosylmethionine. *Plant J.* **44**: 718–729.
- Schultz, C.J., and Coruzzi, G.M. (1995). The aspartate aminotransferase gene family of *Arabidopsis* encodes isoenzymes localized to three distinct subcellular compartments. *Plant J.* **7**: 61–75.
- Sekowska, A., and Danchin, A. (2002). The methionine salvage pathway in *Bacillus subtilis*. *BMC Microbiol.* **2**: 8.
- Sekowska, A., Dénervaud, V., Ashida, H., Michoud, K., Haas, D., Yokota, A., and Danchin, A. (2004). Bacterial variations on the methionine salvage pathway. *BMC Microbiol.* **4**: 9.
- Shen, W., Nada, K., and Tachibana, S. (2000). Involvement of polyamines in the chilling tolerance of cucumber cultivars. *Plant Physiol.* **124**: 431–439.
- Stadler, R., and Sauer, N. (1996). The *Arabidopsis thaliana AtSUC2* gene is specifically expressed in companion cells. *Bot. Acta* **109**: 299–306.
- Stadler, R., Wolf, K., Hilgarth, C., Tanner, W., and Sauer, N. (1995). Subcellular localization of the inducible *Chlorella* HUP1 monosaccharide-H⁺ symporter and cloning of a Co-induced galactose-H⁺ symporter. *Plant Physiol.* **107**: 33–41.
- Stadler, R., Wright, K.M., Lauterbach, C., Amon, G., Gahrtz, M., Feuerstein, A., Oparka, K.J., and Sauer, N. (2005). Expression of GFP-fusions in *Arabidopsis* companion cells reveals non-specific protein trafficking into sieve elements and identifies a novel post-phloem domain in roots. *Plant J.* **41**: 319–331.

- Takahashi, H., Watanabe-Takahashi, A., Smith, F.W., Blake-Kalff, M., Hawkesford, M.J., and Saito, K.** (2000). The roles of three functional sulphate transporters involved in uptake and translocation of sulphate in *Arabidopsis thaliana*. *Plant J.* **23**: 171–182.
- Truernit, E., and Sauer, N.** (1995). The promoter of the *Arabidopsis thaliana* SUC2 sucrose-H⁺ symporter gene directs expression of β -glucuronidase to the phloem: Evidence for phloem loading and unloading by SUC2. *Planta* **196**: 564–570.
- Wilkie, S.E., Lambert, R., and Warren, M.J.** (1996). Chloroplastic aspartate aminotransferase from *Arabidopsis thaliana*: An examination of the relationship between the structure of the gene and the spatial structure of the protein. *Biochem. J.* **319**: 969–976.
- Yamaguchi, K., Takahashi, Y., Berberich, T., Imai, A., Miyazaki, A., Takahashi, T., Michael, A., and Kusano, T.** (2006). The polyamine spermine protects against high salt stress in *Arabidopsis thaliana*. *FEBS Lett.* **580**: 6783–6788.